SIMULATION STUDIES OF ADIABATIC THERMAL BEAMS IN A PERIODIC SOLENOIDAL FOCUSING FIELD*

C. Chen[#], T.J. Barton, D.M. Field and K.M. Lang, MIT, Cambridge, MA 02139, U.S.A.

Abstract

Two-dimensional (2D) particle-in-cell (PIC) simulations are performed to verify earlier theoretical predictions of adiabatic thermal beams in a periodic solenoidal magnetic focusing field. In particular, results are obtained for adiabatic thermal beams that do not rotate in the Larmor frame. For such beams, the theoretical predictions of the rms beam envelope, the conservations of rms thermal emittances, the adiabatic equation of state, and the Debye length are verified in the PIC simulations.

INTRODUCTION

Adiabatic thermal beam equilibrium was discovered recently in a periodic solenoidal magnetic focusing field [1-3]. In particular, the existence of the adiabatic thermal beam equilibrium was shown in the frameworks of kinetic theory and equivalent warm-fluid theory.

In the warm-fluid theory of the adiabatic thermal beam equilibrium [1,2], warm-fluid equations were solved in the paraxial approximation. The equation of state was adiabatic. The rms beam envelope, the density and flow velocity profiles, and the self-consistent Poisson equation were derived.

In the kinetic theory of the adiabatic thermal beam equilibrium [3], the thermal beam distribution function was constructed using the approximate and exact invariants of motion, i.e., a scaled transverse Hamiltonian and the angular momentum. By taking statistical averages, all of the equations in the warm-fluid theory were recovered, including the adiabatic equation of state, the rms beam envelope, the density and flow velocity profiles, and the self-consistent Poisson equation.

Effects of the beam perveance, emittance and rotation on the beam envelope and density distribution were examined. Good agreement was found [3] between theory and a recent high-intensity beam experiment performed at the University of Maryland Electron Ring (UMER) [4].

The phase space for charged-particle motion in the adiabatic thermal beam equilibrium was analyzed [5] and compared with that of the KV-type beam equilibrium [6-8]. It was found that the widths of nonlinear resonances in the adiabatic thermal beam equilibrium are narrower than those in the KV-type beam equilibrium. Numerical evidence is presented, indicating the almost complete absence of chaotic particle motion in the adiabatic thermal beam equilibrium.

The discovery of the adiabatic thermal beam equilibrium was an important advance in beam physics,

_____

overcoming the shortcoming of the Kapchinskij-Vladmirskij (KV) type equilibrium in a periodic solenoidal magnetic focusing field [6-8]. The KV type equilibrium has a singular (δ – function) distribution in the four-dimensional phase space. Such a δ – function distribution gives a uniform density profile across the beam in the transverse directions, and a transverse temperature profile which peaks on axis and decreases quadratically to zero on the edge of the beam. Because of the singularity in the distribution functions, these beam equilibria are not likely to occur in real physical systems and cannot provide realistic models for theoretical and experimental studies and simulations except in the zero-temperature limit. For example, the KV equilibrium model cannot be used to explain the beam tails in the radial distributions observed in the recent high-intensity beam experiment [4]. In contrast, the measured density distribution matches that of the adiabatic thermal beam equilibrium [3,4].

In this paper, results of two-dimensional (2D) particle-in-cell (PIC) simulations are presented, which further validate the theoretical predictions of the adiabatic thermal beam equilibrium. In particular, results are obtained for adiabatic thermal beams that do not rotate in the Larmor frame. For such beams, the theoretical predictions of the rms beam envelope, the conservations of rms thermal emittances, the adiabatic equation of state, and the Debye length are verified in the simulations.

PARTICLE-IN-CELL MODEL

We study charged-particle dynamics in the adiabatic thermal equilibrium of an intense charged-particle beam propagating with constant axial velocity $\beta_b c \hat{\mathbf{e}}_z$ in the periodic solenoidal magnetic focusing field

$$\mathbf{B}^{ext} = B_z(s)\hat{\mathbf{e}}_z - \frac{1}{2}\frac{dB_z(s)}{ds}(x\hat{\mathbf{e}}_x + y\hat{\mathbf{e}}_y), \quad (1)$$

where $s = z$ is the axial coordinate, $B_z(s+S) = B_z(s)$ is the axial magnetic field, S is the fundamental periodicity length of the focusing field, and c is the speed of light in vacuum.

The paraxial approximation is made under the following assumptions : 1) $r_{brms} \ll S$, where r_{brms} is the rms beam radius, and 2) $\nu/\gamma_b^3\beta_b^2 \ll 1$, where $\nu = q^2 N_b/mc^2$ is the Budker parameter of the beam, q and m are the particle charge and rest mass, respectively, $N_b = \int_0^\infty n_b(r,s)2\pi r dr =$ const is the number of charged particles per unit axial length, and $\gamma_b = (1-\beta_b^2)^{-1/2}$ is the relativistic mass factor.

The basic equations in the 2D PIC model are expressed in cgs units as [3]

$$\frac{d^2\widetilde{\mathbf{x}}_{\perp i}}{ds^2} + \kappa_z(s)\widetilde{\mathbf{x}}_{\perp i} + \frac{q}{\gamma_b^3 m\beta_b^2 c^2}\frac{\partial\phi(\widetilde{\mathbf{x}}_{\perp i},s)}{\partial\widetilde{\mathbf{x}}_{\perp i}} = 0\,, \quad (2)$$

$$\frac{\partial\phi(\widetilde{\mathbf{x}}_{\perp i},s)}{\partial\widetilde{\mathbf{x}}_{\perp i}} = -4\pi q n_b(\widetilde{\mathbf{x}}_{\perp i},s)\,, \quad (3)$$

where $i = 1,2,\cdots,N_P$, $\sqrt{\kappa_z(s)} = qB_z(s)/2\gamma_b m\beta_b c^2$, ϕ is the electrostatic potential, n_b is the beam density, and $\widetilde{\mathbf{x}}_{\perp i}$ is the transverse position of the i th macroparticle in the Larmor frame, i.e., $\widetilde{x} = x\cos\varphi - y\sin\varphi$ and $\widetilde{y} = x\sin\varphi + y\cos\varphi$ with $\varphi = \int_0^s \sqrt{\kappa_z(s)}ds$.

In the 2D PIC simulations, the focusing field is chosen to be sinusoidal with $S\sqrt{\kappa_z(s)} = \sigma_0[1 + \cos(2\pi s/S)]$, where σ_0 is the vacuum phase advance. Poisson's equation (3) is solved using a successive over relaxation (SOR) algorithm in a grounded circular perfect conducting pipe of radius R centered on the z-axis on a square mesh. The value of R is chosen to be several times that the maximum value of the rms beam radius.

The 2D PIC simulations discussed in this paper are limited to a class of adiabatic thermal beams that do not rotate in the Larmor frame. For such a class of beams, the macroparticles are loaded at $s = 0$ according to the initial distribution function

$$f(\widetilde{\mathbf{x}}_\perp,\widetilde{\mathbf{x}}'_\perp,s=0) = n_b(\widetilde{r},0)\exp\left\{-\frac{\gamma_b m\beta_b^2\widetilde{\mathbf{x}}'^2_\perp}{2k_BT_\perp(0)}\right\}, \quad (4)$$

where $\widetilde{r} = (\widetilde{x}^2 + \widetilde{y}^2)^{1/2}$, prime denotes derivative with respect to s, k_B is the Boltzmann constant, and $T_\perp(0)$ and $n_b(\widetilde{r},0)$ are the initial beam temperature and density, respectively. The density $n_b(\widetilde{r},0)$ is given by

$$n_b(\widetilde{r},0) = \frac{4\pi C\varepsilon_{th}^2}{r_{brms}^2(0)}\exp\left\{-\frac{K\widetilde{r}^2}{8\varepsilon_{th}^2} - \frac{\widetilde{r}^2}{r_{brms}^2(0)} - \frac{q\phi(\widetilde{r},0)}{\gamma_b^2 k_BT_\perp(0)}\right\}, \quad (5)$$

where C is a constant determined by $N_b = \int_0^\infty n_b(\widetilde{r},s)2\pi\widetilde{r}d\widetilde{r}$, $K \equiv 2q^2N_b/\gamma_b^3 m\beta_b^2 c^2$ is the generalized beam perveance, the initial electrostatic potential $\phi(\widetilde{r},0)$ is determined from the Poisson equation

$$\frac{1}{\widetilde{r}}\frac{\partial}{\partial\widetilde{r}}\left(\widetilde{r}\frac{\partial}{\partial\widetilde{r}}\right)\phi(\widetilde{r},0) = -4\pi q n_b(\widetilde{r},0)\,, \quad (6)$$

and $r_{brms}(0)$ and $r'_{brms}(0) = 0$ are the initial conditions of the periodic rms beam envelope $r_{brms}(s) = r_{brms}(s+S)$ that solves the rms beam envelope equation

$$\frac{d^2 r_{brms}}{ds^2} + \kappa_z(s)r_{brms} - \frac{K}{2r_{brms}} = \frac{4\varepsilon_{th}^2}{r_{brms}^3}\,. \quad (7)$$

The trajectories of the macroparticles are integrated using the standard leapfrog method.

The 2D PIC algorithm is implemented in a Matlab version of the MIT 2D Periodically Focused Beam (PFB2D) code which was used extensively in simulation studies of high-brightness charged-particle beams in periodic focusing fields [9]. The trajectories of the macroparticles are integrated using the standard leapfrog method.

RESULTS

Two-dimensional PIC simulations are performed to verify the theoretical predictions on the following:

a)   rms beam envelope;
b)   conservations of rms thermal emittances;
c)   adiabatic equation of state;
d)   density, velocity, and temperature profiles; and
e)   Debye length.

Results of a typical PFB2D simulation are shown in Figs. 1-5 for the parameters: $\sigma_0 = 80°$, $SK/4\varepsilon_{th} = 7.0$, $N_P = 1\times10^6$, $(S/4\varepsilon_{th})^{1/2}R = 5.0$, integration step size $\Delta s/S = 0.01$, and mesh size $(S/4\varepsilon_{th})^{1/2}\Delta\widetilde{x} = 0.02$.

The focusing parameter $S^2\kappa_z(s) = \sigma_0^2[1 + \cos(2\pi s/S)]^2$ is plotted in Fig. 1 as a function of the normalized distance s/S . The normalized rms beam radius $(S/4\varepsilon_{th})^{1/2}r_{brms}$ from the PFB2D simulation is plotted in Fig. 2 as a function of the normalized distance s/S . Within the statistical error of $\pm1\%$, the result agrees with the matched beam envelope solution of Eq. (7).
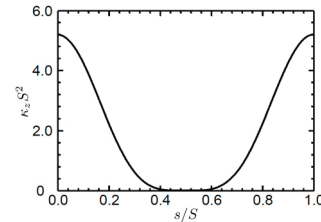

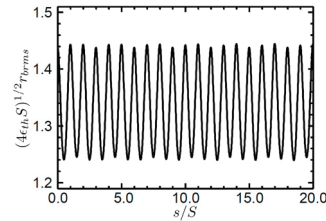Figure 1: Plot of the normalized focusing parameter $S^2\kappa_z(s)$ versus the normalized distance s/S .

Figure 2: Plot of the normalized rms beam radius $(S/4\varepsilon_{th})^{1/2}r_{brms}$ versus the normalized distance s/S .
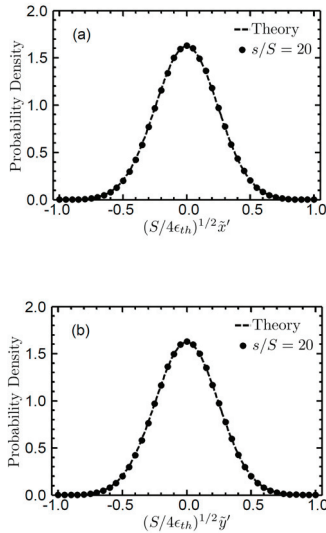
Figure 3: Plots of (a) probability density distributions $\rho(\tilde{x}')$ versus $(S/4\varepsilon_{th})^{1/2}\tilde{x}'$ and (b) probability density distributions $\rho(\tilde{y}')$ versus $(S/4\varepsilon_{th})^{1/2}\tilde{y}'$ at $s/S = 20$. The dotted curves are from the PFB2D simulation, whereas the dashed curves are from the theoretical predictions [1-3].
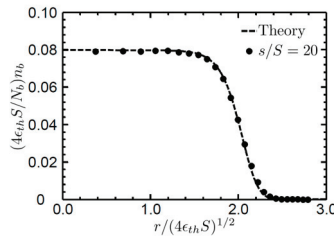
Figure 4: Plot of the normalized beam density $(4\varepsilon_{th}S/N_b)n_b$ versus the normalized radius $(S/4\varepsilon_{th})^{1/2}r$ at $s/S = 20$.
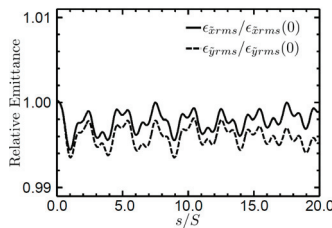
Figure 5: Plots of the relative rms thermal emittances $\varepsilon_{\tilde{x}rms}/\varepsilon_{\tilde{x}rms}(0)$ and $\varepsilon_{\tilde{y}rms}/\varepsilon_{\tilde{y}rms}(0)$ versus the normalized distance s/S.

The transverse momentum distribution remains to be Gaussian, as illustrated in Fig. 3. It is evident that there is good agreement between the simulation and theory.

The beam density distribution maintains a plateau distribution as shown in Fig. 4 in which the normalized beam density $(4\varepsilon_{th}S/N_b)n_b$ is plotted as a function of the normalized radius $(S/4\varepsilon_{th})^{1/2}r$ at $s/S = 20$. The dotted curves are from the PFB2D simulation, whereas the dashed curves are from the theoretical predictions. The characteristic scale over which the beam density falls is the Debye length λ_D [1-3], which, in this example, has a normalized value of $(S/4\varepsilon_{th})^{1/2}\lambda_D = 0.14$. There is good agreement between the simulation and theory.

In Fig. 5, the evolutions of the relative rms thermal emittances $\varepsilon_{\tilde{x}rms}/\varepsilon_{\tilde{x}rms}(0)$ and $\varepsilon_{\tilde{y}rms}/\varepsilon_{\tilde{y}rms}(0)$ in the PFB2D simulation are shown in solid and dashed curves, respectively, as a function of s/S. Here, $\varepsilon_{\tilde{x}rms}(0)$ and $\varepsilon_{\tilde{y}rms}(0)$ are the rms thermal emittances in the $\tilde{x}$- and $\tilde{y}$-directions at $s = 0$, respectively. Both rms emittances are conserved within the statistical error of $\pm0.3\%$. These results are in agreement with the theoretical predictions of the conservations of rms thermal emittances and adiabatic equation of state.

CONCLUSION

Two-dimensional particle-in-cell simulations were performed to verify the theoretical predictions of adiabatic thermal beams in a periodic solenoidal magnetic focusing field. Results were obtained for adiabatic thermal beams that do not rotate in the Larmor frame. For such beams, the theoretical predictions of the rms beam envelope, the conservations of rms thermal emittances, the adiabatic equation of state, and the Debye length were verified in the 2D PIC simulations.

REFERENCES

[1] K. R. Samokhvalova, J. Zhou, and C. Chen, Phys. Plasmas **14**, 103102 (2007).

[2] K. R. Samokhvalova, *Thermal Equilibrium Theory of Periodically Focused Charged-Particle Beams*, Ph.D Thesis, Massachusetts Institute of Technology, 2008.

[3] J. Zhou, K. R. Samokhvalova, and C. Chen, Phys.Plasmas **15**, 023102 (2008).

[4] S. Bernal, B. Quinn, M. Reiser, and P.G. O'Shea, Phys. Rev. ST Accel. Beams **5**, 064202 (2002).

[5] H. Wei and C. Chen, Phys. Rev. ST. Accel. Beams **14**, 024201 (2011).

[6] I.M. Kapchinskij and V.V. Vladimirskij, in Proc. Conf. High Energy Accel. (CERN, Geneva, 1959), p. 274.

[7] C. Chen, R. Pakter, and R. C. Davidson, Phys. Rev. Lett. **79**, 225 (1997).

[8] R. C. Davidson and H. Qin, *Physics of Intense Charged Particle Beams in High Energy Accelerators* (Imperial College Press, Singapore, 2001), p. 242.

[9] J. Zhou, R. Bhatt, and C. Chen, Phys. Rev. ST. Accel. Beams **9**, 034401 (2006).

05 Beam Dynamics and Electromagnetic Fields

D04 High Intensity in Linear Accelerators